Yahong Chen*, Jing Wang and Ruoya Wang

Crystal structure of 7-(diethylamino)-3-(benzoyl)-2*H*-chromen-2-one, $C_{20}H_{19}NO_3$

https://doi.org/10.1515/ncrs-2024-0426
Received October 30, 2024; accepted December 22, 2024;
published online January 13, 2025

Abstract

$C_{20}H_{19}NO_3$, orthorhombic, $P2_12_12_1$ (no. 19), a = 8.2965(7) Å, b = 12.5111(11) Å, c = 16.2899(15) Å, V = 1,690.9(3) Å^3, Z = 4, $R_{gt}(F)$ = 0.0582, $wR_{ref}(F^2)$ = 0.1257, T = 298.8(6) K.

CCDC no.: 2394920

Table 1 contains crystallographic data and Table 2 contains the list of the atoms including atomic coordinates and displacement parameters (Figure 1).

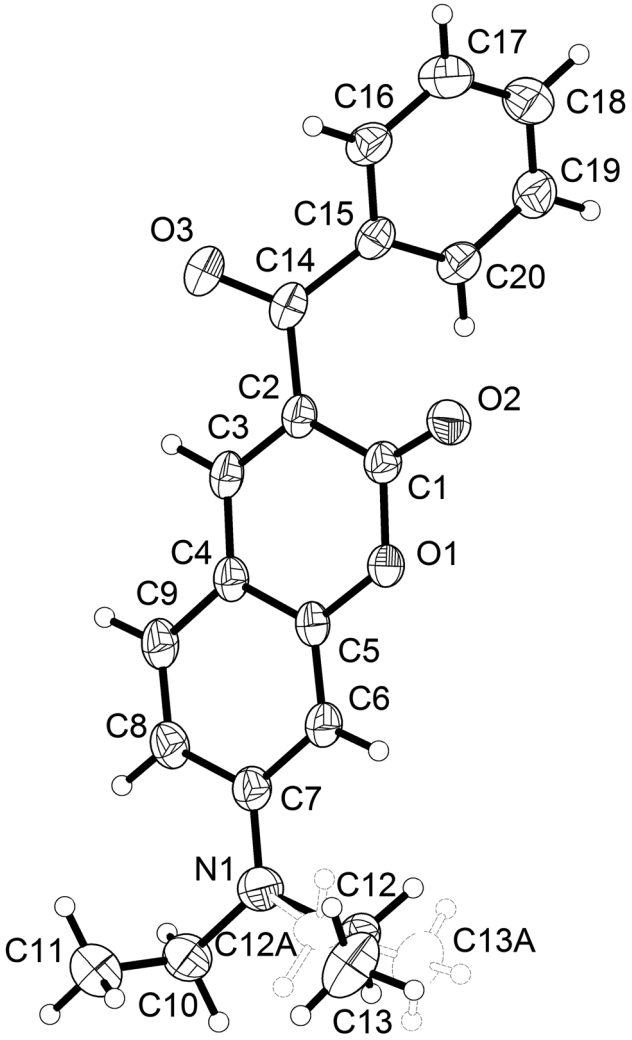

1 Source of material

The title compound, 7-(diethylamino)-3-(benzoyl)-2*H*-chromen-2-one was synthesized according to the literature methodology with slight modification.[5,6] Ethanol was selected as the solvent for the condensation between 4-diethylaminosalicylaldehyde and ethyl benzoylacetate. The synthetic efficiency is dependend on the reaction temperature. In a 100 mL round bottom flask, 4-diethylaminosalicylaldehyde (580 mg, 3 mmol) and ethyl benzoylacetate (635 mg, 3.3 mmol) were mixed with 50 mL anhydrous ethanol. Subsequently, piperidine (0.02 mmol) was added and the reaction mixture was refluxed for about 1 h. The reaction was monitored with the methodology of thin layer chromatography (TLC). Once one of the starting 4-diethylaminosalicylaldehyde disappeared completely on the TLC plate, the reaction was quenched by adding distilled water 20 mL. The obtained mixture was extracted with dichloromethane (30 mL × 3) and washed with distilled water (30 mL × 3). Then, the organic phase was dried over $MgSO_4$. The volatile components was evaporated on the rotary evaporating equipment. The residue was purified by column chromatography on silica gel (dichloromethane/ethyl acetate). The crystal cultivation was carried in saturated ethanol solution into a NMR tube. After slow evaporation, suitable crystal was selected for X-ray diffraction and data was collected.

2 Experimental details

Hydrogen atoms attached to C atoms were placed geometrically and refined using a riding model approximation, with d(C–H) = 0.93 Å, 0.97 Å, or 0.96 Å (–CH, $-CH_2$, $-CH_3$). U_{iso}(H) = 1.2 U_{eq}(C) for CH or U_{iso}(H) = 1.5 U_{eq}(C) for CH_3 and

***Corresponding author: Yahong Chen**, College of Chemistry and Chemical Engineering, Zhoukou Normal University, Zhoukou, 466000, P.R. China, E-mail: chenyahong@zknu.edu.cn
Jing Wang and Ruoya Wang, College of Chemistry and Chemical Engineering, Zhoukou Normal University, Zhoukou, 466000, P.R. China

Table 1: Data collection and handling.

Crystal:	Yellow block
Size:	0.40 × 0.33 × 0.20 mm
Wavelength:	Mo *K*α radiation (0.71073 Å)
μ:	0.09 mm^{-1}
Diffractometer, scan mode:	SuperNova, ω
θ_{max}, completeness:	28.8°, >99 %
$N(hkl)_{measured}$, $N(hkl)_{unique}$, R_{int}:	7,335, 3,613, 0.028
Criterion for I_{obs}, $N(hkl)_{gt}$:	$I_{obs} > 2\sigma(I_{obs})$, 2,547
$N(param)_{refined}$:	239
Programs:	CrysAlis^{PRO},[1] Olex,[2] SHELX[3,4]

Table 2: Fractional atomic coordinates and isotropic or equivalent isotropic displacement parameters (Å^2).

Atom	*x*	*y*	*z*	U_{iso}*/U_{eq}
O1	0.5960 (3)	0.30724 (17)	0.30668 (15)	0.0554 (6)
O2	0.6893 (3)	0.2786 (2)	0.18312 (16)	0.0675 (7)
O3	0.5977 (4)	0.5845 (2)	0.11298 (18)	0.0821 (9)
N1	0.4405 (5)	0.3510 (3)	0.5843 (2)	0.0825 (11)
C1	0.6165 (4)	0.3402 (3)	0.2263 (2)	0.0497 (8)
C2	0.5563 (4)	0.4453 (2)	0.2051 (2)	0.0474 (8)
C3	0.4900 (4)	0.5076 (2)	0.2649 (2)	0.0510 (9)
H3	0.456502	0.576282	0.251262	0.061*
C4	0.4700 (4)	0.4731 (2)	0.3456 (2)	0.0484 (8)
C5	0.5268 (4)	0.3707 (2)	0.3661 (2)	0.0487 (8)
C6	0.5195 (4)	0.3292 (3)	0.4435 (2)	0.0574 (9)
H6	0.559808	0.261226	0.454081	0.069*
C7	0.4510 (4)	0.3894 (3)	0.5070 (2)	0.0571 (9)
C8	0.3900 (4)	0.4921 (3)	0.4876 (2)	0.0591 (10)
H8	0.341653	0.532927	0.528428	0.071*
C9	0.4011 (4)	0.5320 (3)	0.4098 (2)	0.0599 (10)
H9	0.361872	0.600237	0.399162	0.072*
C10	0.3706 (5)	0.4111 (4)	0.6518 (2)	0.0754 (12)
H10A	0.338839	0.361474	0.694580	0.090*
H10B	0.274020	0.446713	0.632396	0.090*
C11	0.4816 (6)	0.4928 (4)	0.6879 (3)	0.0980 (15)
H11A	0.515043	0.541796	0.645826	0.147*
H11B	0.574463	0.457868	0.710561	0.147*
H11C	0.426425	0.531311	0.730440	0.147*
C12[a]	0.4570 (10)	0.2334 (6)	0.6001 (5)	0.063 (2)
H12A[a]	0.443710	0.193083	0.549713	0.076*
H12B[a]	0.377357	0.209421	0.639633	0.076*
C13[b]	0.6248 (11)	0.2202 (9)	0.6337 (7)	0.104 (3)
H13A[b]	0.700954	0.250836	0.596006	0.156*
H13B[b]	0.647760	0.145596	0.640664	0.156*
H13C[b]	0.632781	0.255902	0.685676	0.156*
C14	0.5767 (4)	0.4884 (3)	0.1210 (2)	0.0556 (9)
C15	0.5654 (4)	0.4200 (3)	0.0470 (2)	0.0486 (8)
C16	0.6523 (4)	0.4483 (3)	−0.0221 (2)	0.0621 (10)
H16	0.722248	0.506287	−0.020369	0.074*
C17	0.6351 (5)	0.3904 (4)	−0.0938 (3)	0.0774 (12)
H17	0.696314	0.408329	−0.139612	0.093*
C18	0.5285 (6)	0.3066 (4)	−0.0980 (3)	0.0801 (12)
H18	0.515150	0.269261	−0.146857	0.096*
C19	0.4420 (5)	0.2785 (3)	−0.0298 (3)	0.0681 (11)
H19	0.369893	0.221632	−0.032354	0.082*
C20	0.4613 (4)	0.3342 (3)	0.0430 (2)	0.0573 (9)
H20	0.403858	0.313629	0.089428	0.069*
C12A[c]	0.5790 (16)	0.2675 (8)	0.6114 (6)	0.076 (3)
H12C[c]	0.668820	0.269977	0.573305	0.091*
H12D[c]	0.618231	0.283890	0.666004	0.091*
C13A[d]	0.5018 (17)	0.1616 (8)	0.6098 (8)	0.107 (4)
H13D[d]	0.444283	0.152874	0.559126	0.161*
H13E[d]	0.428068	0.155701	0.654982	0.161*
H13F[d]	0.582868	0.107132	0.614311	0.161*

[a]Occupancy: 0.527(9), [b]occupancy: 0.55, [c]occupancy: 0.437(9), [d]occupancy: 0.45.

CH_2 groups.[3] One of the ethyl groups attached to nitrogen atom is positionally disordered and rotates around the nitrogen atom. Therefore, it was split to parts with 53 and 47 %, separately. SADI command was used to refine with identical bond length. The anisotropic refinement of C13 was restricted by ISOR command due to its larger thermal ellipsoids.

3 Comment

7-(Diethylamino)-3-(benzoyl)-2*H*-chromen-2-one is attractive due to coumarin-containing configuration and strong fluorescencing character. Therefore, many fluorescent probes, bio-markers, solar cells, etc. were developed based on the coumarin core structure.[7–11] The title compound with a build in electron donor (diethylamino) and electron acceptor (carbonyl) configured the strong intramolecular electron push-pull system. Together with the specifically π system of coumarin, an easily modifiable fluorescence emission could be developed. Based on this strategy, the fluorescence emission maximum can be shifted to longer wavelength (red region).[12,13] Bright emitting devices were fabricated by doping fluorescent derivatives.

In the title crystal structure, the asymmetric unit contains one molecule. Both the bond lengths and the angles are in the expected ranges. The core coumarin part is coplanar with the root mean square error (RMSD) in distance estimated to be 0.020 Å. Other groups, ethyl, carbonyl, and benzene, are twisted out of the plane of coumarin. The distance of C2–C14 is determined to be 1.482(5) Å and shorter than that of the saturated carbons. However, the carbonyl is not coplanar with the coumarin and therefore the two parts are not conjugated. Vice versa, the distance of N1–C7 is estimated to be 1.351(5) Å, which is shorter than the distance of N1–C10 (1.453 Å) and N1–C12 (1.500 Å). It demonstrates that

the N1 conjugated with the coumarin framework, which can effectively donate the electron toward the coumarin moiety. Therefore, the donor (NEt_2) and carbonyl group generates a strong intramolecular "push-pull" effect. Based on this "push-pull" electronic effect, the emission performance could be modified effectively.[14–18] Additionally, the amino structure (N1/C7/C10/C12 or N1/C7/C10/C12A) does not construct the ideal trigonal pyramid geometry but complanar with the RMSD in distance 0.053 Å for N1/C7/C10/C12 and 0.093 Å for N1/C7/C10/C12A, respectively. It indicates that there exists the electron donation character of N1 in some degree. The adjacent parallel molecules are fixed by the C–H···π interactions. The hydrogen atoms (H13A/H13B/H13F, H16, and H8/H9) are located directly above the benzene ring (C4/C5/C6/C7/C8/C9 and C15/C16/C17/C18/C19/C20). The H···centroid distance ranges from 2.97 to 3.95 Å, which is well inside the interval classified to 2.65 to 4.0 Å.[19] The C–H bonds point to the ring carbon rings center and corresponds to a type III, VI, and V geometry. Besides the C–H···π interactions mentioned above, typical C–H···O interactions also found in the adjacent nonparallel molecules. The distances of C···O distances are 3.260–3.396 Å (C12···O1 and C13···O3), which is well inside the interval of 3.0–4.0 Å quoted by Desiraju.[20] The angles between C12–H12B···O1 and C13–H13A···O3 are 153.3 and 130.8°, which is also in agreement with the above mentioned survey.[20,21] The hydrogen bond investigation is beneficial to analyse the solid emission behavior of fluorescent dye molecules.[22–25] The introduction of oxygen atoms is the key factor for the configuration of inter- or intra-molecular hydrogen bonds. The excited state of dye molecules is highly dependend on the intermolecular interactions, which determines the ration between radiative and nonradiative channels.[26] When there exist highly stronger intramolecular interactions, the significant fluorescence quench will not be avoided.[27–30]

The crystal lattices were mainly stabilized by the hydrogen bonds and C–H···π interactions. Only two hydrogens (H12B and H13A) were involved in the establishment of hydrogen bonds, which jointed the adjacent molecules side by side. It should be noted that there are no π···π interactions established in the crystal lattice. Both the hydrogen bonds and C–H···π interactions analyzed above are weak intramolecular interactions, which facilitate the emission performance in solid state.[31] Without the establishment of π···π interaction, parallel-displaced conformation also was not observed, which may lead to regular tight packing model and quench the fluorescence emission.[32–36] The non-radiative channel can be enhanced owing to the regular parallel packing model.[37,38] To the crystal of 7-(diethylamino)-3-(benzoyl)-2*H*-chromen-2-one, the weak interaction, together with the intramolecular electron "push-pull" effect, leads to the character of strong emission.[39–41] In conclusion, the molecules are staggered layer by layer along the axis *b*, and H···O contact joints the layers. Both the bond lengths and the angles are in the expected ranges.[42–44]

Acknowledgments: We gratefully thank Prof. Xiaochuan Li (Henan Normal University) for provding lab facilities and supporting the X-ray diffraction data acquisition and structure solving.
Author contributions: All the authors have accepted responsibility for the entire content of this submitted manuscript and approved submission.
Research funding: None declared.
Conflict of interest: The authors declare no conflicts of interest regarding this article.

References

1. Oxford Diffraction Ltd. CrysAlis^{PRO}, Abingdon, Oxfordshire, England, 2006.
2. Dolomanov, O. V.; Bourhis, L. J.; Gildea, R. J.; Howard, J. A. K.; Puschmann, H. OLEX^2: A Complete Structure Solution, Refinement and Analysis Program. *J. Appl. Cryst.* 2009, *42*, 339–341.
3. Sheldrick, G. M. Crystal Structure Refinement with *SHELXL*. *Acta Crystallogr.* 2015, *C71*, 3–8.
4. Sheldrick, G. M. *SHELXTL*—Integrated Space-Group and Crystal-Structure Determination. *Acta Crystallogr.* 2015, *A71*, 3–8; https://journals.iucr.org/a/issues/2015/01/00/sc5086/index.html.
5. Secci, D.; Carradori, S.; Bolasco, A.; Chimenti, P.; Yanez, M.; Ortuso, F.; Alcaro, S. Synthesis and Selective Human Monoamine Oxidase Inhibition of 3-Carbonyl, 3-Acyl, and 3-Carboxyhydazido Coumarin Derivatives. *Eur. J. Med. Chem.* **2011**, *46*, 4846–4852.
6. Specht, D. P.; Martic, P. A.; Farid, S. A New Class of Triplet Sensitizers. *Tetrahedron* **1982**, *38*, 1203–1211.
7. Zheng, X.; Liu, X.; Liu, L.; Li, X.; Jiang, S.; Niu, C.; Xie, P.; Liu, G.; Cao, Z.; Ren, Y.; Qin, Y.; Wang, J. Multi-Stimuli-Induced Mechanical Bending and Reversible Fluorescence Switching in a Single Organic Crystal. *Angew. Chem., Int. Ed.* **2022**, *61*, e202113073.
8. Li, X.; Han, Y.; Sun, S.; Shan, D.; Ma, X.; He, G.; Mergu, N.; Park, J.-S.; Kim, C.-H.; Son, Y.-A. A Diaminomaleonitrile-Appended BODIPY Chemosensor for the Selective Detection of Cu^{2+} via Oxidative Cyclization and Imaging in SiHa Cells and Zebrafish. *Spectrochim. Acta, Part A* **2020**, *233*, 118179.
9. Cui, D.; Zhang, L.; Zhang, J.; Li, W.; Chen, J.; Guo, Z.; Sun, C.; Wang, Y.; Wang, W.; Li, S.; Huang, W.; Zheng, C.; Chen, R. Hybrid Local and Charge-Transfer Material with Ultralong Room Temperature Phosphorescence for Efficient Organic Afterglow Light-Emitting Diodes. *Angew. Chem., Int. Ed.* **2024**, *63*, e202411588.
10. Li, X.; Liu, X.; Li, F. Configuration of Super-Fast Cu^{2+}-Responsive Chemosensor by Attaching Diaminomaleonitrile to BODIPY Scaffold for High-Contrast Fluorescence Imaging of Living Cells. *Spectrochim. Acta, Part A* **2024**, *304*, 123377.
11. Xie, P.; Zhou, Y.; Li, X.; Liu, X.; Liu, L.; Cao, Z.; Wang, J.; Zheng, X. Strong Dual-State Emission of Unsymmetrical and Symmetrical Thiazolothiazole-Bridged Imidazolium Salts. *Chin. Chem. Lett.* **2023**, *34*, 107582.

12. Li, X.; Han, Y.; Kim, M.; Son, Y. A. A BODIPY-Based Highly Emissive Dye with Thiophene-Based Branch Harvesting the Light. *Mol. Cryst. Liq. Cryst.* **2018**, *662*, 157–164.
13. Liu, Y.; Li, X.; Min, K. S.; Son, Y. A. Highly Fluorescent Response of 4-(2,5-Dimethylthiophen-3-yl)-2-Hydroxyphenylbenzothiazole toward $BF_3{\cdot}Et_2O$ and Zn^{2+}. *Mol. Cryst. Liq. Cryst.* **2018**, *662*, 132–138.
14. Li, X.; Li, F.; Ji, G. A Fluorescent Turn-On Sensor toward Multiple Heavy Metal Ions Based on Meso-Anisole Modified BODIPY Scaffold. *J. Fluoresc.* **2023**, *33*, 631–637.
15. Li, Y.; Liu, K.; Zhang, W.; Wang, Y.; Wang, B.; Wang, Y.; Li, X. Two 3D Ln(III)-mOFs Based on Phosphineoxide Ligand: Synthesis, Structure Luminescent and Photocatalytic Properties. *J. Fluoresc.* **2023**, *33*, 2119–2129.
16. Zhu, X.; Feng, L.; Cao, S.; Wang, J.; Niu, G. Donor–Acceptor–Acceptor-Conjugated Dual-State Emissive Acrylonitriles: Investigating the Effect of Acceptor Unit Order and Biological Imaging. *Org. Lett.* **2022**, *24*, 8305–8309.
17. Cao, Z.; Yang, F.; Wu, D.; Wu, L.; Liu, L.; Liu, G.; Li, X.; Zheng, X.; Zheng, X.; Qu, D. Supramolecular Aggregates Constructed by Pillar [5]arene-Based Host–Guest Interaction with Aggregation-Induced Emission. *Polym. Chem.* **2023**, *14*, 1318–1322.
18. Li, X.; Yao, C.; Jiang, W. Emission and Energy Transfer Investigation of Non-conjugated Total Carbon Configuration between BODIPY and Naphthalimide. *J. Chem. Sci.* **2023**, *135*, 65.
19. Malone, J. F.; Murray, C. M.; Charlton, M. H.; Docherty, R.; Lavery, A. J.: X–H$\cdots\pi$ (Phenyl) Interactions Theoretical and Crystal Lo Graphic Observations. *J. Chem. Soc. Faraday Trans.* **1997**, *93*, 3429–3436.
20. Desiraju, G. R. The C–H$\cdots$O Hydrogen Bond in Crystals: What Is It? *Acc. Chem. Res.* **1991**, *24*, 290–296.
21. Steiner, T. The Hydrogen Bond in the Solid State. *Angew. Chem., Int. Ed.* **2002**, *41*, 48–76.
22. Li, X.; Qian, Q.; Jiang, W. Photo-induced Fluorochromism of a Star-Shaped Photochromic Dye with 2,4-Dimethylthiazole Attaching to Triangle Terthiophene. *J. Fluoresc.* **2023**, *33*, 1907–1915.
23. Ji, G.; Hou, Q.; Jiang, W.; Li, X. Investigating the Properties of Double Triangle Terthiophene Configured Dumbbell-like Photochromic Dye with Ethyne and 1,3-butadiene Bridge. *J. Fluoresc.* **2023**, *33*, 1495–1503.
24. Li, X.; Zou, Y.; Heo, G.; Son, Y. A. Emission Shift of an Imidazole Bridged Diethylaminocoumarin and Diphenyl. *Mol. Cryst. Liq. Cryst.* **2020**, *704*, 48–56.
25. Li, X.; Tian, G.; Shao, D.; Xu, Y.; Wang, Y.; Ji, G.; Ryu, J.; Son, Y. A. A BODIPY Based Emission Signal Turn-On Probe toward Multiple Heavy Metals. *Mol. Cryst. Liq. Cryst.* **2020**, *706*, 38–46.
26. Liu, Y.; Li, X.; Min, K. S.; Son, Y. A. Emission Behavior of Naphthalimide-Coumarin Cassette. *Mol. Cryst. Liq. Cryst.* **2018**, *662*, 139–146.
27. Janiak, C. A Critical Account on π–π Stacking in Metal Complexes with Aromatic Nitrogen-Containing Ligands. *J. Chem. Soc. Dalton. Trans.* **2000**, *21*, 3885–3896.
28. Li, X.; Liao, M.; Sun, J.; Heo, G.; Son, Y. A. Thiophene Modulated BODIPY Dye as a Light Harvester. *Mol. Cryst. Liq. Cryst.* **2019**, *679*, 127–136.
29. Li, X.; Guo, X.; Chen, Y.; Cui, T.; Xing, L. Double 3-Ethyl-2,4-Dimethylpyrrole Configured Fluorescent Dye with Fluorine-Boron as the Bridge. *J. Fluoresc.* **2021**, *31*, 1797–1803.
30. Liu, Y.; Li, X.; Kim, H.; Son, Y. A. Investigation of Fluorescent Optical Properties of Fluorine-Boron Cored Dye. *Mol. Cryst. Liq. Cryst.* **2018**, *677*, 27–33.
31. Ji, G.; Hou, Q.; Zhang, J.; Li, X. Investigation of Triangle Terthiophene and Hydroxyphenylbenzothiazole Configured Fluorescent Dye with a Triple Bond Bridge. *J. Fluoresc.* **2023**, *33*, 153–159.
32. Li, X.; Cai, Q.; Zhang, J.; Kim, H.; Son, Y. A. An "Electron Lock" toward the Photochromic Activity of Phenylacetylene Appended Bisthienylethene. *Mol. Cryst. Liq. Cryst.* **2020**, *706*, 141–149.
33. Li, X.; Zhou, Q.; Heo, G.; Son, Y. A. 2,4-Dimethylpyrrole Configured Fluorine-Boron Complexes. *Mol. Cryst. Liq. Cryst.* **2018**, *677*, 34–41.
34. He, W.; Li, X.; Kim, H.; Son, Y. A. Shifting the Emission of Proton Transfer Fluorescence with Fluorine-Boron as the Rotation Lock. *Mol. Cryst. Liq. Cryst.* **2020**, *704*, 41–47.
35. Li, X.; Han, Y.; Kim, M. J.; Son, Y. A. Reversed Photochromism Reactivity of Malononitrile Attached Bisthienylthene. *Mol. Cryst. Liq. Cryst.* **2018**, *662*, 147–156.
36. Li, X.; Wang, Y.; Jia, C.; Kim, H.; Son, Y. A. Photochromic Reactivity Induced by Electron Distribution: Active or Inactive. *Mol. Cryst. Liq. Cryst.* **2019**, *689*, 83–91.
37. Ji, G.; Hou, Q.; Jiang, W.; Li, X. Investigating the Properties of Triangle Terthiophene and Triphenylamine Configured Propeller-like Photochromic Dye with Ethyne Bridge. *J. Fluoresc.* **2024**. https://doi.org/10.1007/s10895–023–03557-w, In press.
38. Li, X.; Liu, X. A Sensitive Probe of Meso-Cyanophenyl Substituted BODIPY Derivative as Fluorescent Chemosensor for the Detection of Multiple Heavy Metal Ions. *J. Fluoresc.* **2024**. https://doi.org/10.1007/s10895–024–03581–4, In press.
39. Li, X.; Han, Y.; Min, K.; Son, Y. A. Configuration of White Light Emission by Courmarin and Naphthalimide. *Mol. Cryst. Liq. Cryst.* **2018**, *660*, 10–16.
40. Qian, C.; Xie, L.; Liu, L.; Cao, Z.; Tian, D.; Sun, D.; Liu, G.; Guo, Z.; Zheng, X. Anion-Induced Opposite Mechanochromic and Thermochromic Emission Directions of Protonated Hydrazones. *Sci. China Mater.* **2024**, https://doi.org/10.1007/s40843-024-3169-8, In press.
41. Tian, D.; Lin, J.; Mesbah, A.; Zhou, J.; Yang, M.; Gautier, R.; Chen, X. A Core–Shell Model of Polymetallic Hybrid Metal Halides. *Chem. Commun.* **2024**, *60*, 12924–12927.
42. Liu, Y.; Li, X.; Sun, S.; Ji, G.; Son, Y. A. Crystal Structure of 2,7-Diiodo-1,3,6,8-tetramethyl-bis(difluoroboron)-1,2-bis((1*H*-Pyrrol-2-yl)methylene) hydrazine, $C_{14}H_{14}B_2F_4I_2N_4$. *Z. Kristallogr. N. Cryst. Struct.* **2020**, *235*, 371–372.
43. He, W.; Liu, Y.; Sun, S.; Ji, G.; Li, X. Crystal Structure of 2-Bromo-1,3,6,8-tetramethylBOPHY (BOPHY = Bis(difluoroboron)-1,2-bis((1*H*-pyrrol-2-yl) methylene)hydrazine), $C_{14}H_{15}B_2BrF_4N_4$. *Z. Kristallogr. N. Cryst. Struct.* **2021**, *236*, 949–952.
44. Liu, Y.; Sun, S.; Ji, G.; Li, X.; Son, Y. A. Crystal Structure of 2-Phenylethynyl-1,3,6,8-tetramethylBOPHY (BOPHY = Bis(difluoroboron)-1,2-bis((1*H*-pyrrol-2-yl)methylene)hydrazine), $C_{22}H_{20}B_2F_4N_4$. *Z. Kristallogr. N. Cryst. Struct.* **2021**, *236*, 749–752.